

# WP2

## Thermoelectric Harvesting



Dario Narducci,  
Univ. of Milano Bicocca, Dept. Materials Science  
[dario.narducci@unimib.it](mailto:dario.narducci@unimib.it)

## Outline

Redundant TEG strategies:

- bottom-up, by VLS
- top-down by non-critical lithography

Modeling set up to optimize wire lengths upon heat source characteristics

All technologies are IC-compatible to support integration in the final prototype



## Strategy and device layouts

**Goal:** Obtain all-silicon thermoelectric micronanogenerators by means of the integration of silicon based NW arrays (as thermoelectric material) into a Si micromachined structure able to exploit a waste heat source to develop an internal thermal contrast between two isolated silicon parts.

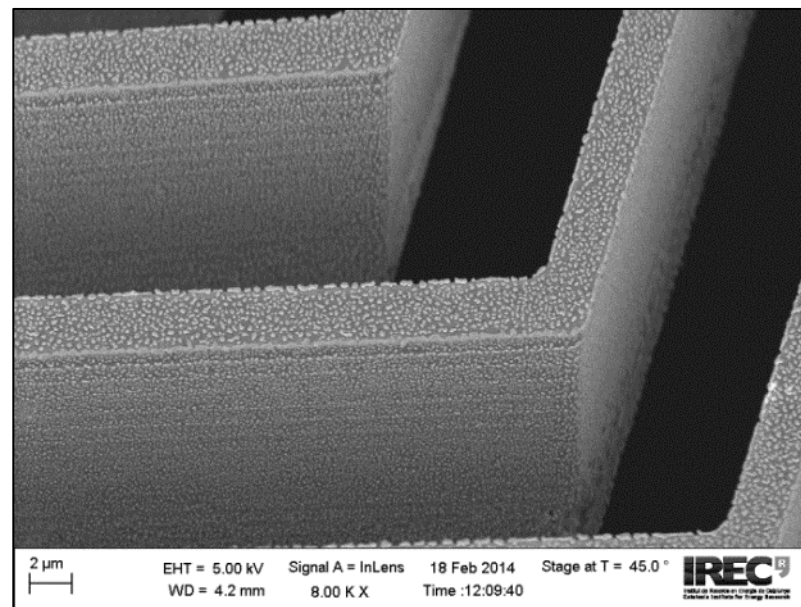
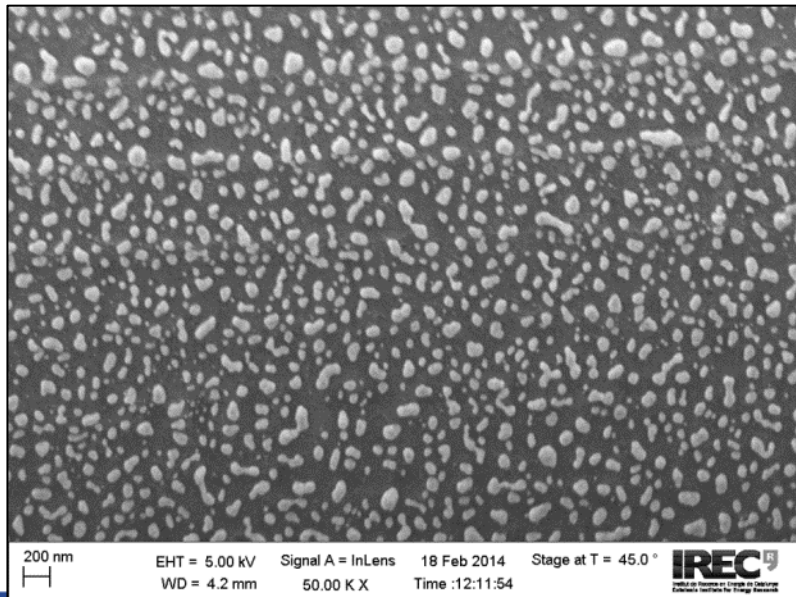
## Bottom-up strategy

NWs will be grown with a VLS-CVD method that allows the in-situ integration of large density arrays of NWs within a 3D structure without specific nanolithography techniques.

# Microemulsion Galvanic Displacement

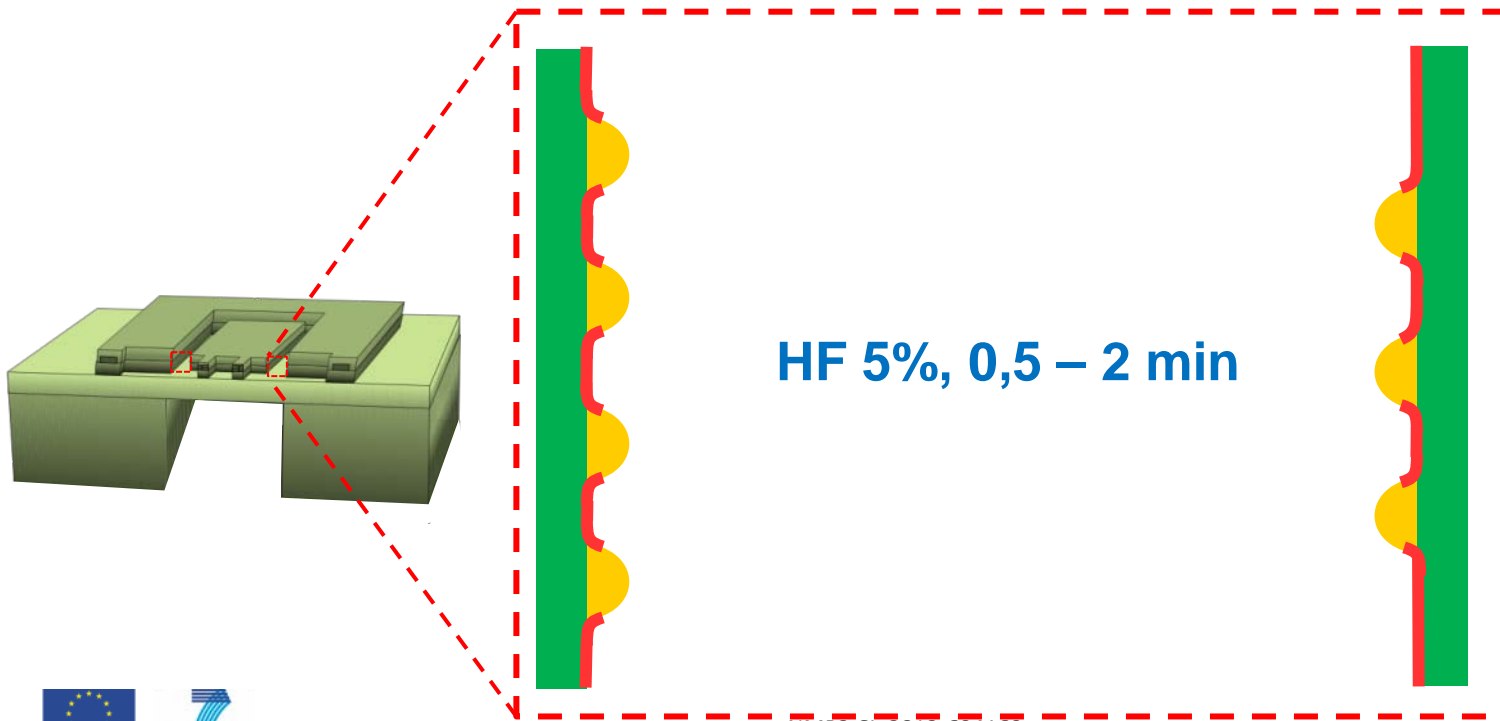
To seed the surface with gold nanoparticles, devices are

1. **dipped in HF** in order to remove native oxide from trenches
2. **dipped in microemulsions** during a controlled dipping time. Gold NPs are formed
3. **annealed** to remove the remaining surfactant



NMP3-SL-2013-604169

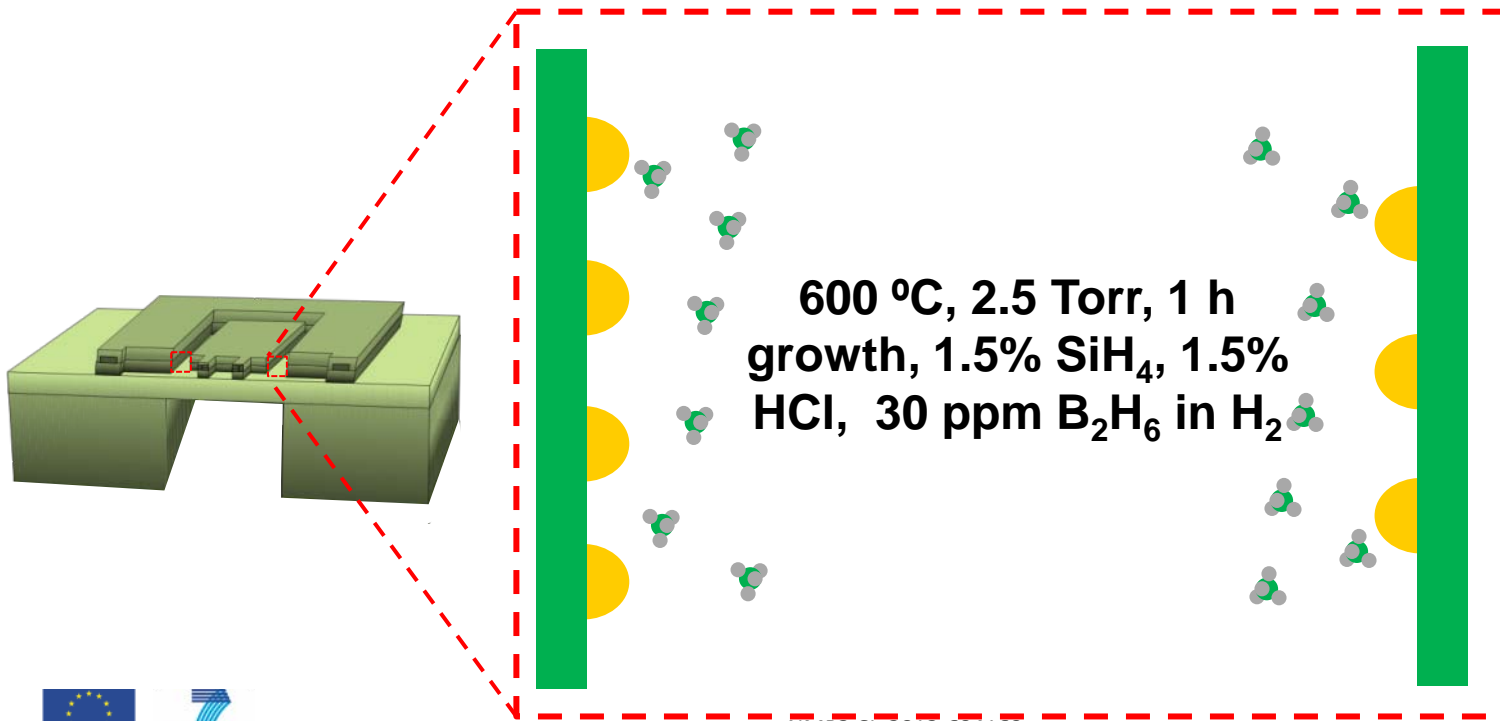
1 – Devices are dipped in **HF** in order to remove thermal oxide formed during calcination



NMP3-SL-2013-604169

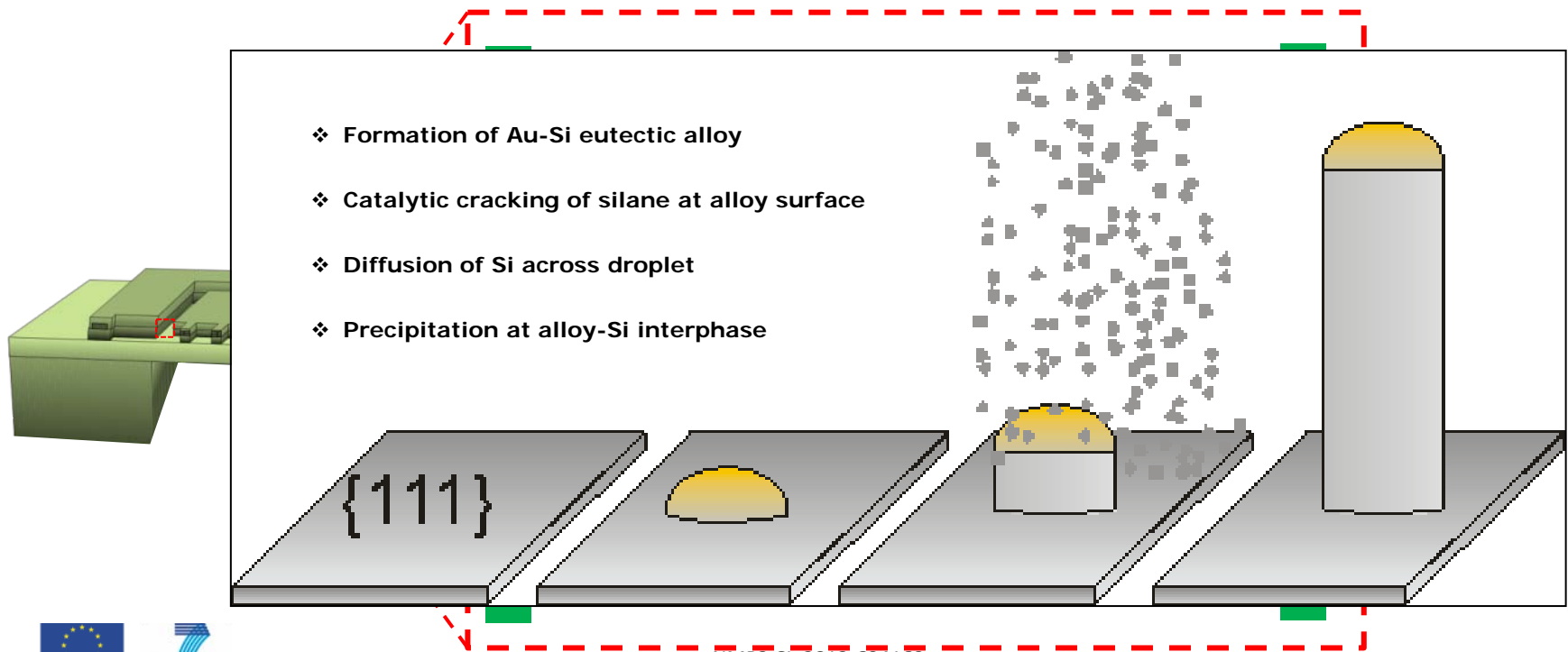
# CVD-VLS growth of NWs

- 1 – Devices are dipped in **HF** in order to remove thermal oxide formed during calcination
- 2 – Devices are loaded into **CVD** and **exposed to silane**. Silicon nanowires are grown by VLS synthesis



NMP3-SL-2013-604169

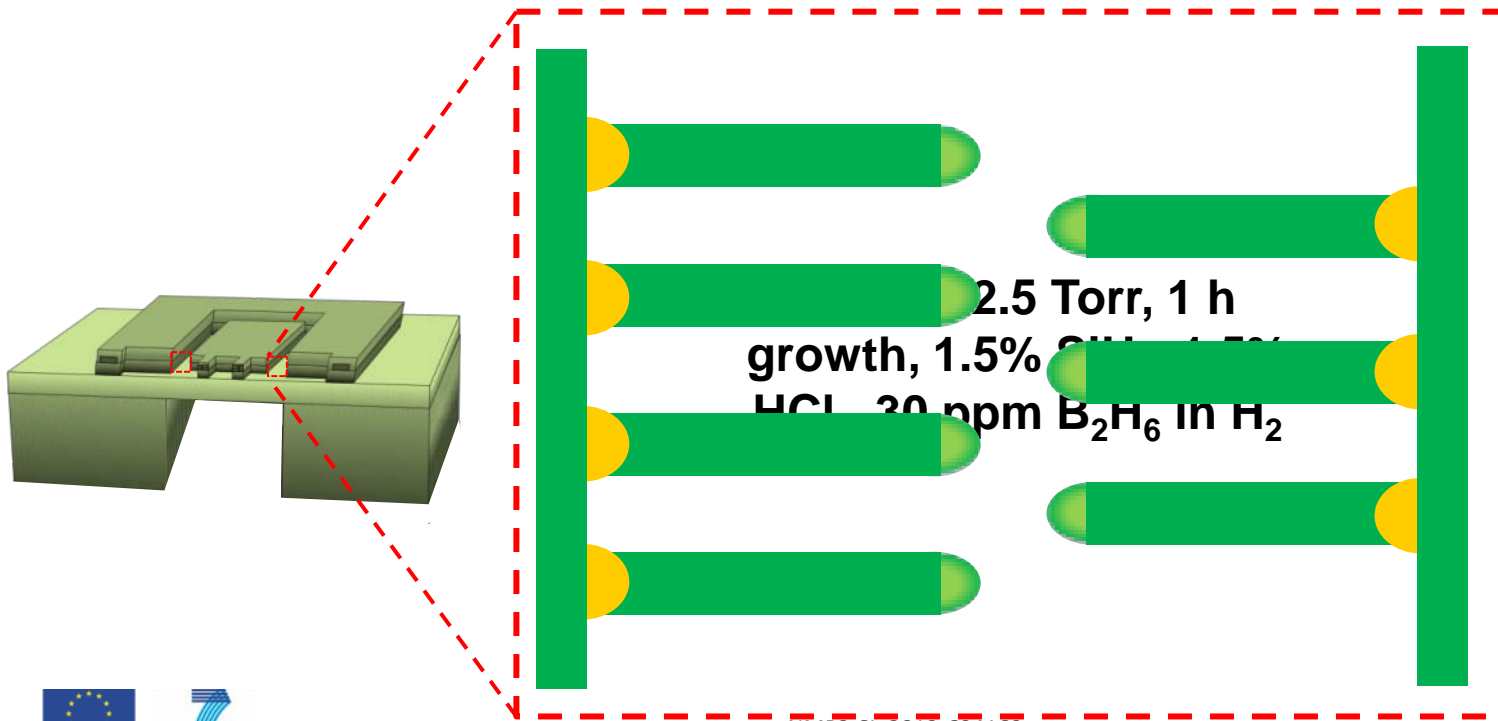
- 1 – Devices are dipped in **HF** in order to remove thermal oxide formed during calcination
- 2 – Devices are loaded into **CVD and exposed to silane**. Silicon nanowires are grown by VLS synthesis





# CVD-VLS growth of NWs

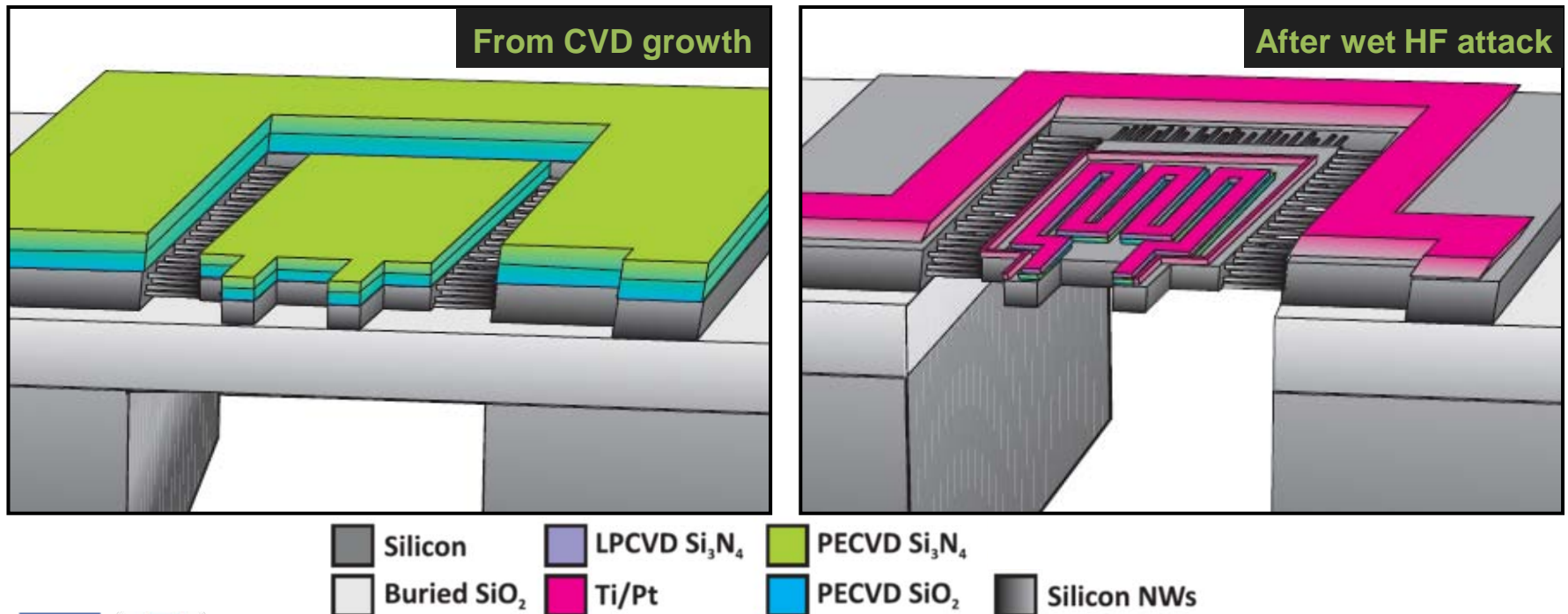
- 1 – Devices are dipped in **HF** in order to remove thermal oxide formed during calcination
- 2 – Devices are loaded into **CVD** and **exposed to silane**. Silicon nanowires are grown by VLS synthesis



NMP3-SL-2013-604169

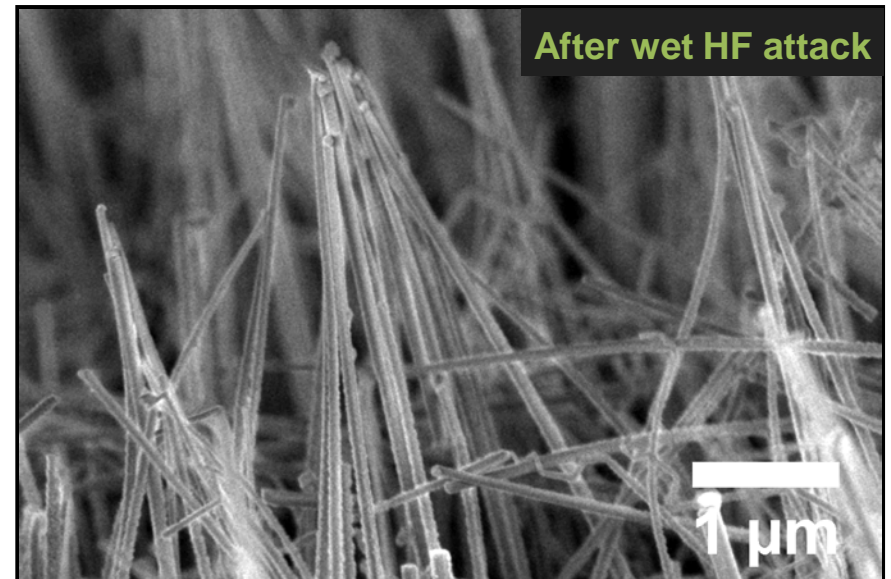
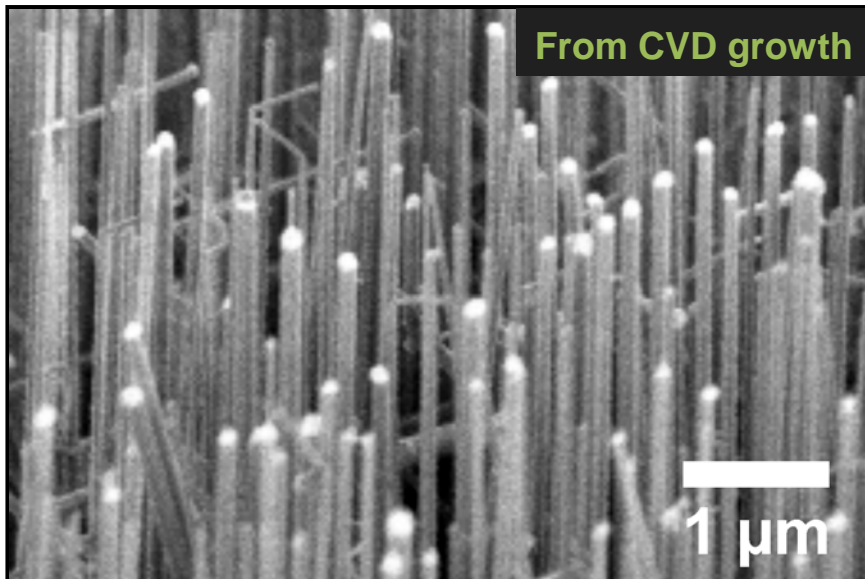
# Membrane removal in HF

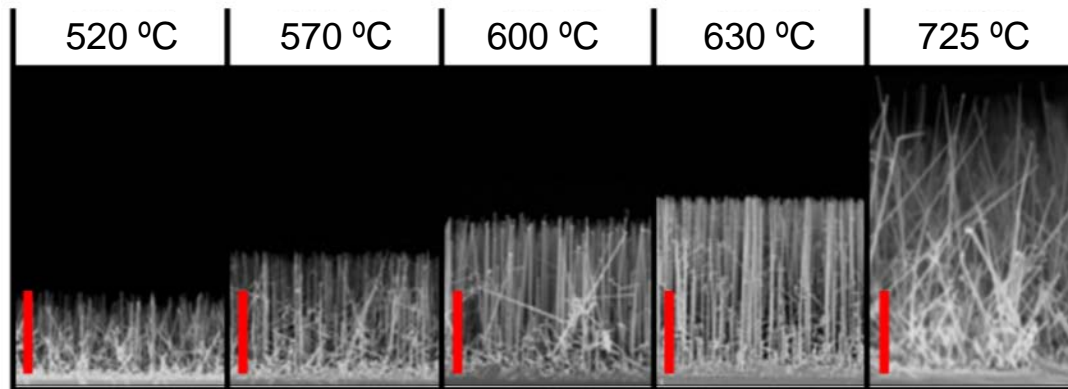
After growing Si NWs in a  $\mu$ TEG device a wet attack in HF must be performed in order to remove membrane and passivation silicon oxide – which covers contacts.



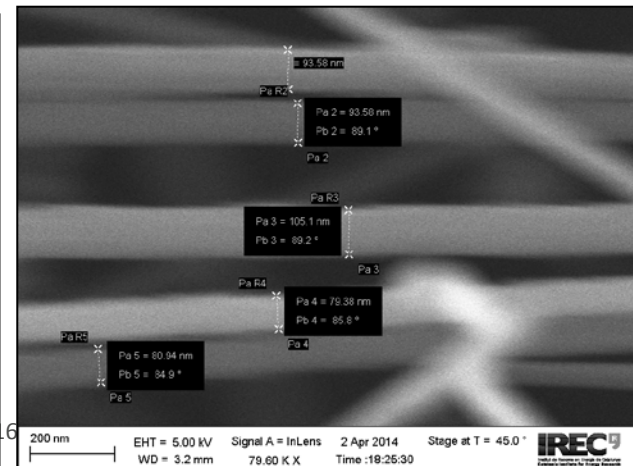
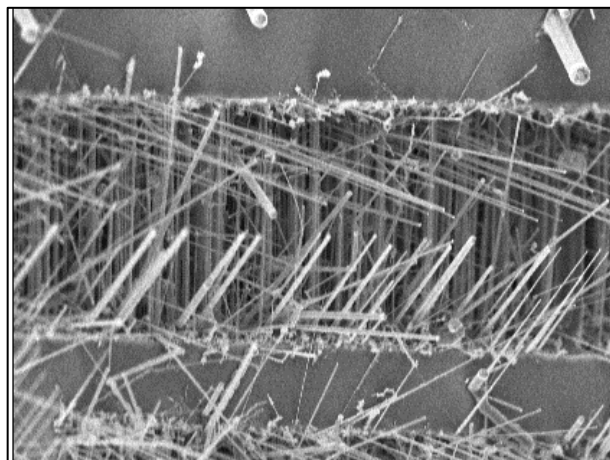
# Membrane removal in HF

After growing Si NWs in a  $\mu$ TEG device a wet attack in HF must be performed in order to remove membrane and passivation silicon oxide – which covers contacts.





- Growth rate increases with T
- Verticality has a maximum in 630 °C
- Well aligned horizontal Si NWs were obtained in trenches

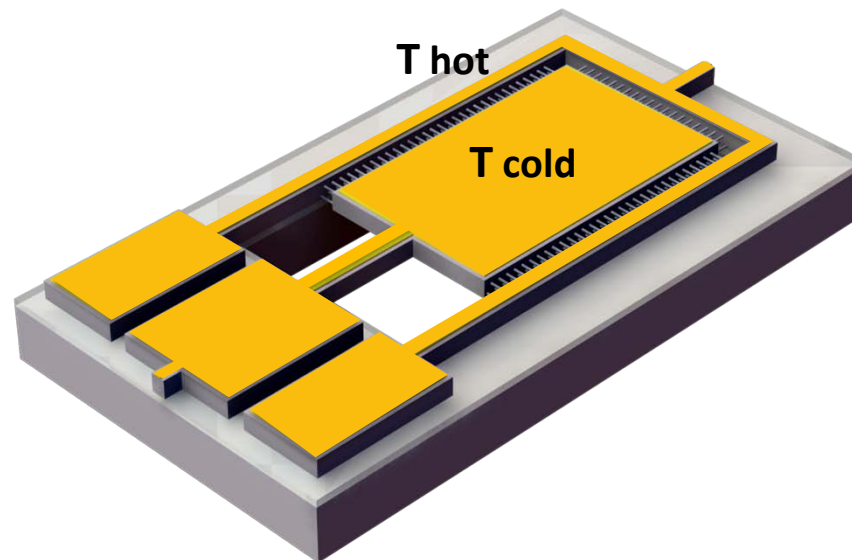


## Bottom-up strategy – Device layout

Structural core will be a Si device micromachined in such a way that hot and cold areas develop when resting on a hot surface.

**Hot area:** surrounding rim **Cold area:** suspended platform.

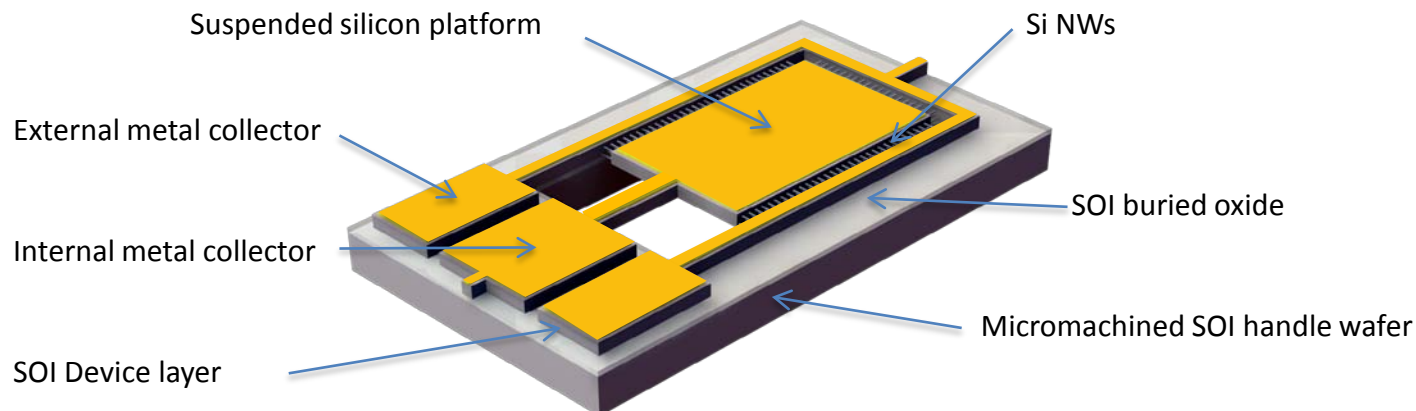
**Thermocouple:** nanostructured silicon and thin metal film.



NMP3-SL-2013-604169

## Bottom-up strategy – Device layout

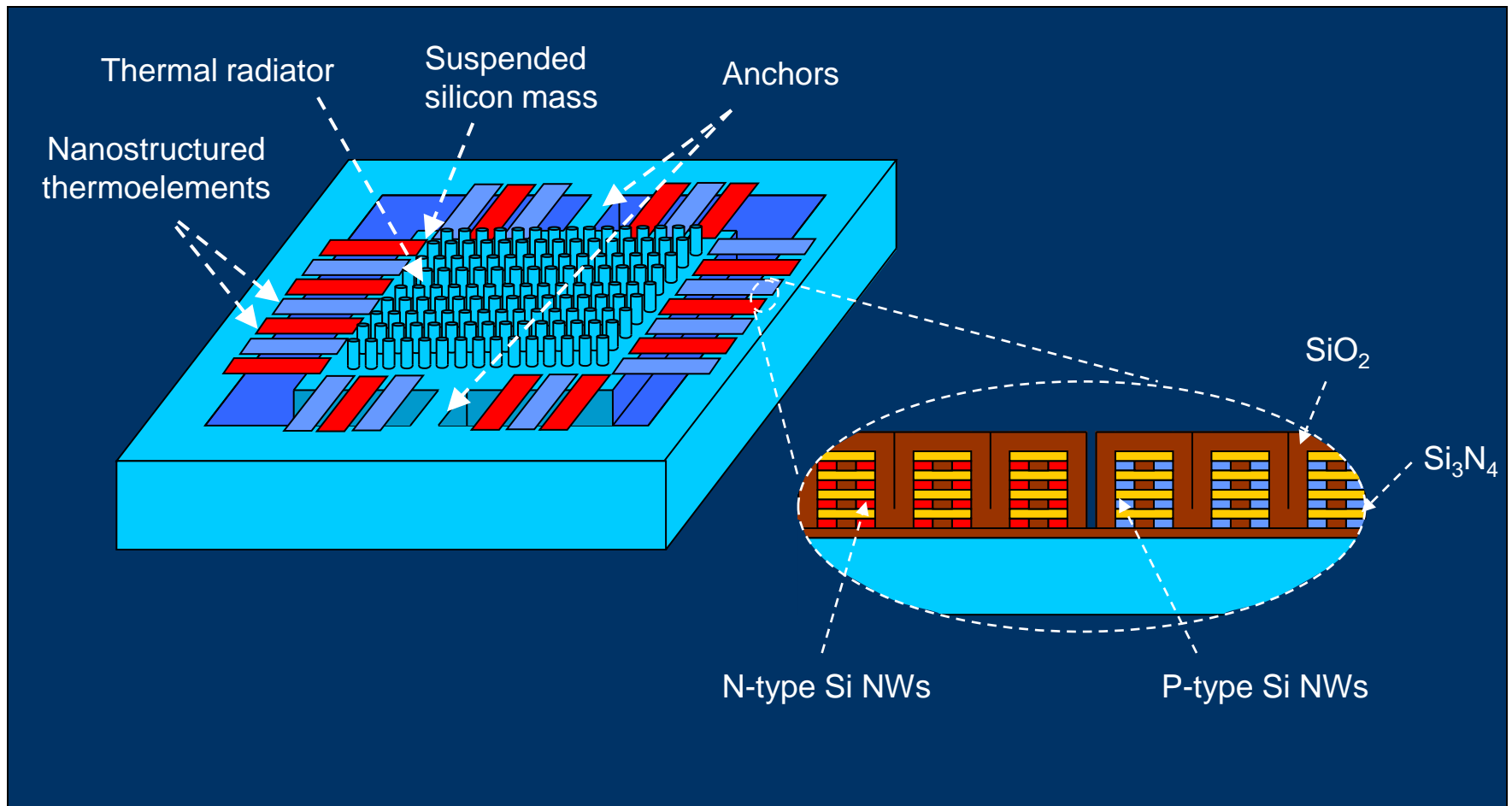
- SOI wafers used as starting material. Device layer  $\langle 110 \rangle$ , so that parallelograms with  $\langle 111 \rangle$  oriented walls can be built .
- Typical size will be 1 mm, with  $10\ \mu\text{m}$  trench widths. Depth is fixed by device layer thickness, which will be around  $10\text{--}15\ \mu\text{m}$  to accommodate a large number of NWs.



## Top-down strategy

NWs will be grown with a CVD method within nanometric cavities built up by controlled etching and filling of recessed regions (without nanolithographic steps).

## Top-down layout with lateral NWs:





# Top-down fabrication of lateral NWs:

1. Si substrate



2. SiO<sub>2</sub> growth



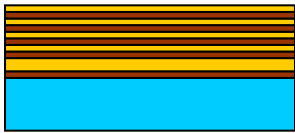
3. Si<sub>3</sub>N<sub>4</sub> deposition



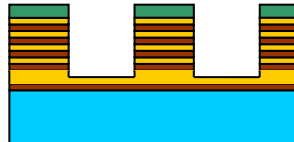
4. SiO<sub>2</sub> deposition



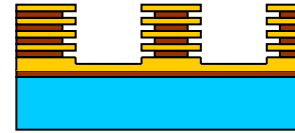
5. Si<sub>3</sub>N<sub>4</sub>/SiO<sub>2</sub> deposition



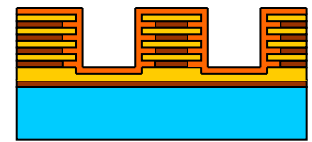
6. Si<sub>3</sub>N<sub>4</sub>/SiO<sub>2</sub> RIE



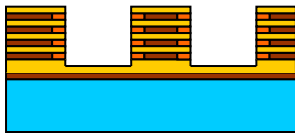
7. SiO<sub>2</sub> wet etching



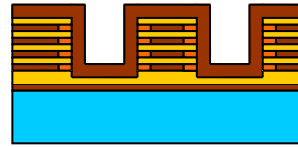
8. Poly deposition



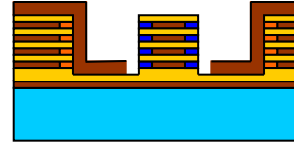
9. Poly etchback



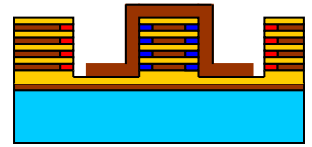
10. SiO<sub>2</sub> deposition



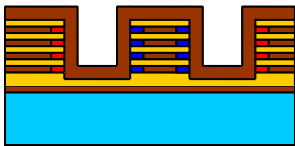
11. P-type doping



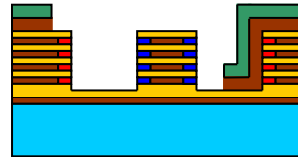
12. N-type doping



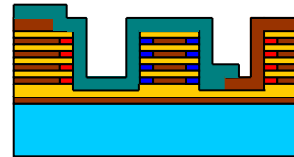
13. SiO<sub>2</sub> deposition



14. SiO<sub>2</sub> etching



15. Al patterning



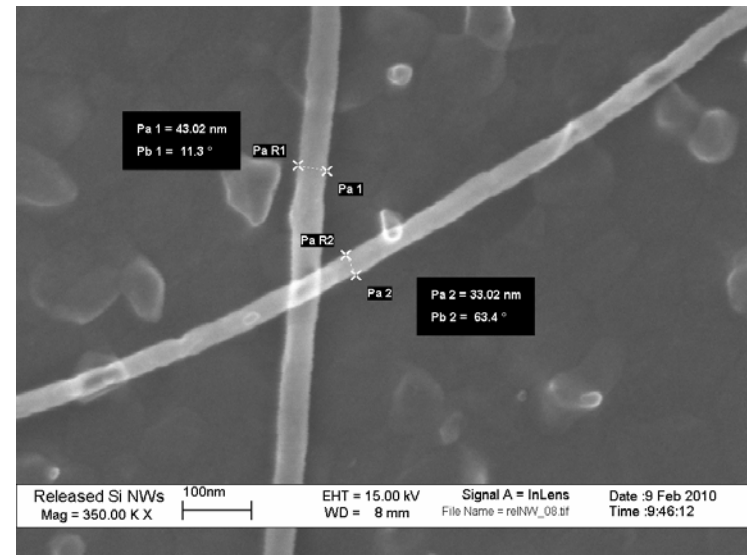
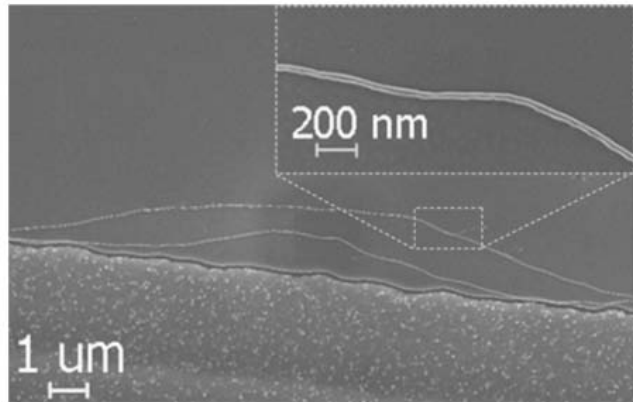
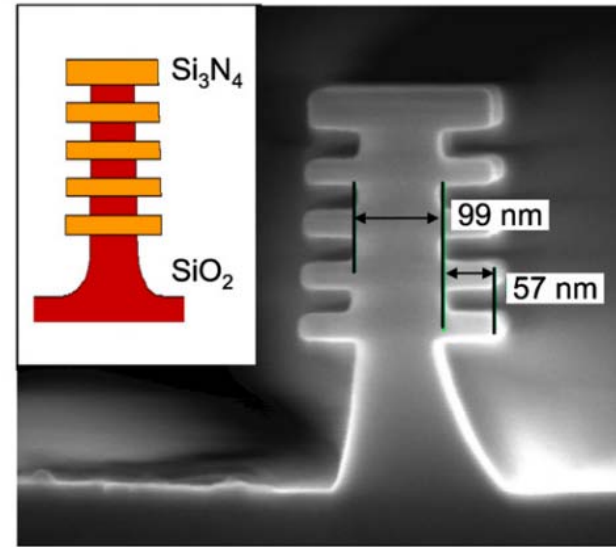
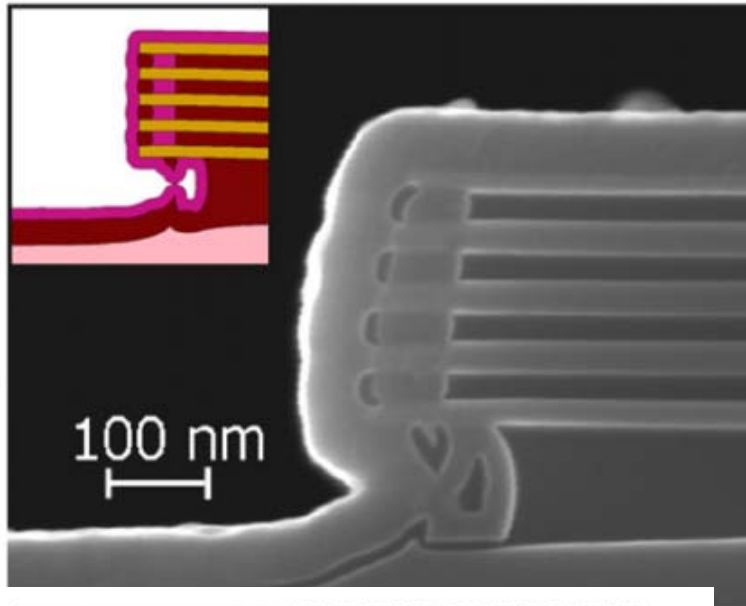


**Fig. 5.** SEM images at different magnifications of the nanowire after detachment from the hosting structure.

## From aims to practice

- NWs have high  $R_{th}$  ( $\approx 10^6 \text{ K W}^{-1}\text{nm}^{-1} / \text{NW}$ )
- For  $\Delta T = 50 \text{ K}$ , max heat acceptance is  $\approx 25 \text{ pW/NW}$  @ wire length of 1 mm
- If  $\eta = 5 \%$  a target power output of  $10 \text{ }\mu\text{W/cm}^2$  requires a wire density of  $10^8 \text{ cm}^{-2}$ , i.e. a wire spacing of about  $1 \text{ }\mu\text{m}$

Critical design issues are:

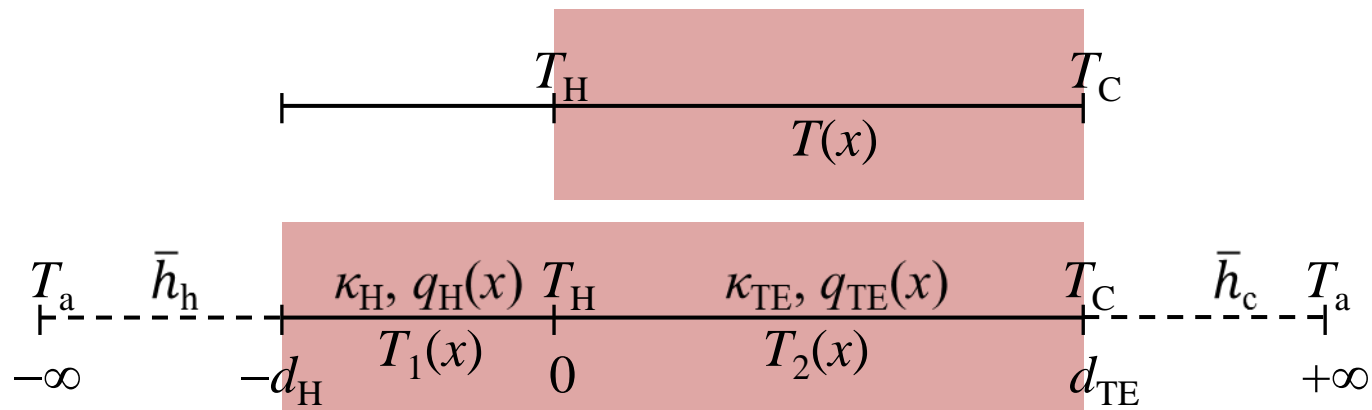
- optimal wire length
- optimal geometry (lateral or vertical)

# The model

Choice of boundary conditions leads to contrasting design indications:

$$W_{el} = W_{th} \eta_{TE} = (\Delta T / R_{th}) \eta_{TE}$$

- setting fixed-T BC's:  $W_{el}$  increases as  $R_{th}$  decreases
- setting fixed-heatflow BC's:  $W_{el}$  increases as  $R_{th}$  increases



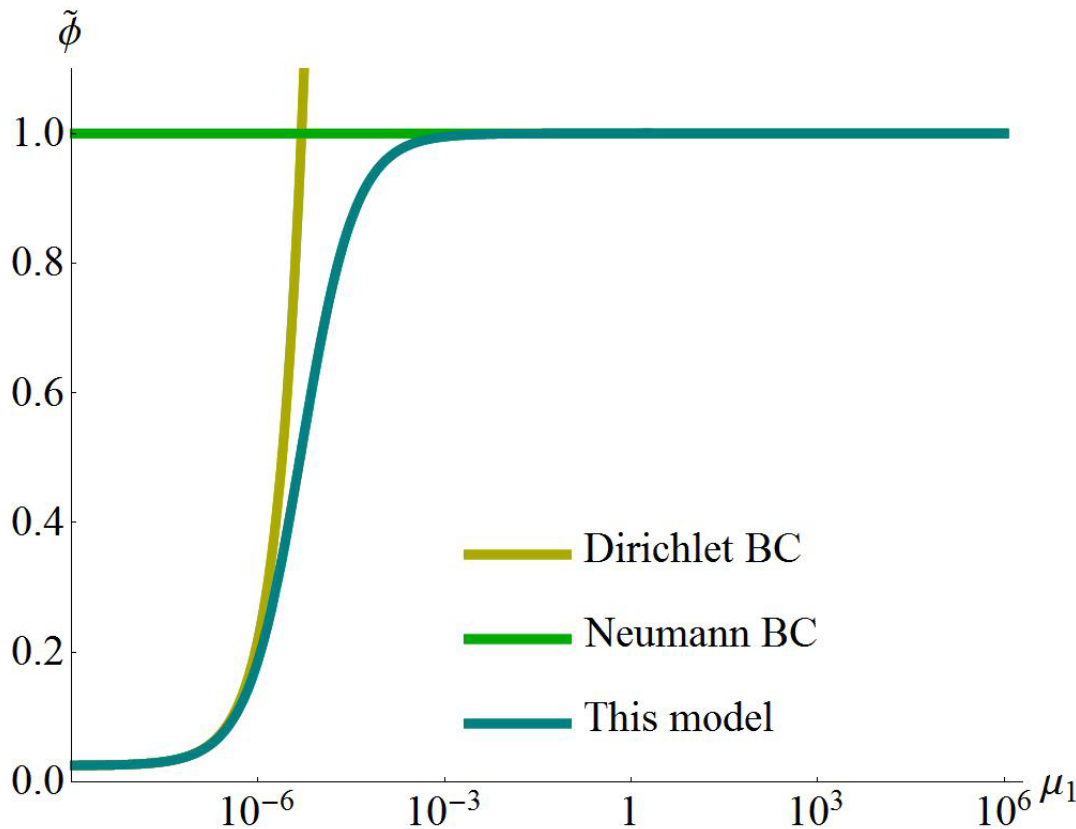
## Model equation

$$\left\{ \begin{array}{l} \kappa_{\text{TE}} T_2''(x) + q_{\text{TE}}(x) = 0 \\ \bar{h}_c (T_2(d_{\text{TE}}) - T_A) = -\kappa_{\text{TE}} T_2'(d_{\text{TE}}) \\ \kappa_{\text{H}} T_1''(x) + q_{\text{H}}(x) = 0 \\ \bar{h}_h (T_1(-d_{\text{H}}) - T_A) = \kappa_{\text{H}} T_1'(-d_{\text{H}}) \\ \kappa_{\text{TE}} T_2'(0) = \kappa_{\text{H}} T_1'(0) \\ T_1(0) = T_2(0) \end{array} \right.$$

$$q_{\text{H}}(x) \equiv \frac{\theta_{\text{H}}}{d_{\text{H}}} \Pi \left( \frac{x}{d_{\text{H}}} + \frac{1}{2} \right) > 0$$

$$q_{\text{TE}}(x) \equiv -\frac{\theta_{\text{TE}}}{d_{\text{TE}}} \Pi \left( \frac{x}{d_{\text{TE}}} - \frac{1}{2} \right) < 0$$

# Reconciling with Neumann and Dirichlet

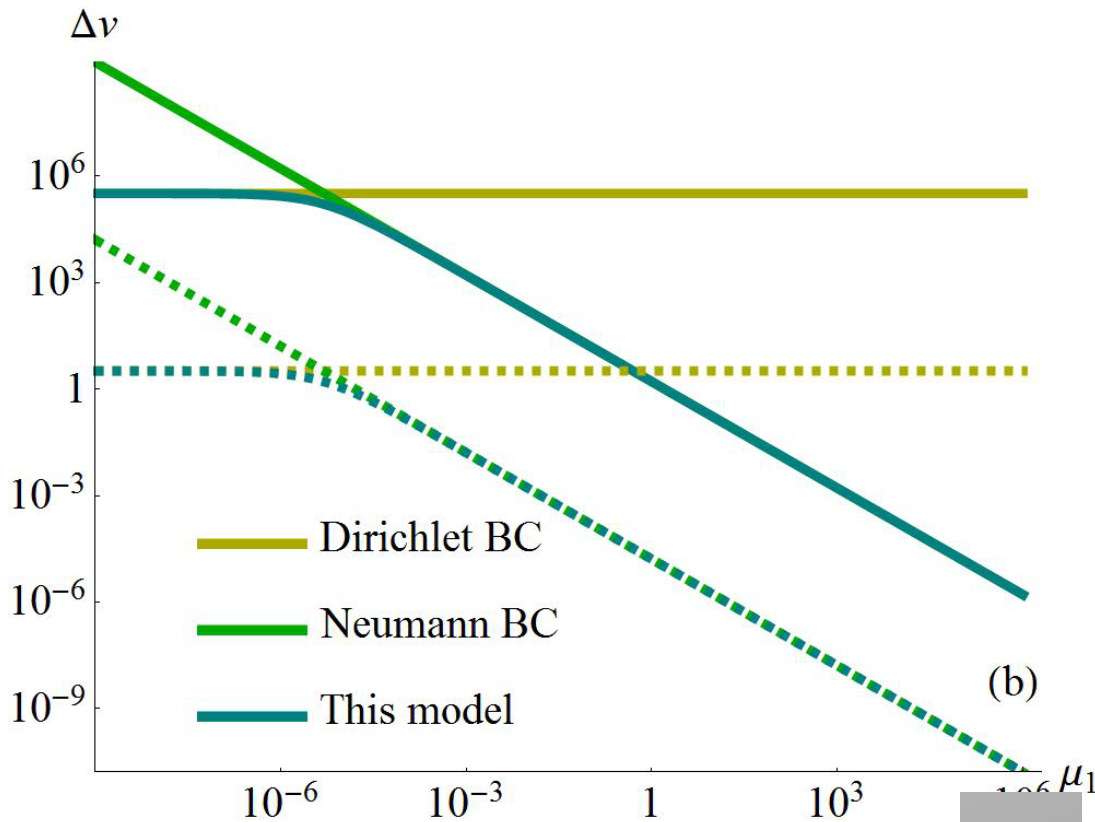


For ideally dissipating cold sides and perfectly insulated heat sources ( $1/\mu_4 = \mu_5 = 0$ ) constant heat flow BCs are recovered for  $\mu_1 > 1$  (Neumann)

$$\mu_1 \equiv d_H / d_{TE}$$

$$\tilde{\phi} \equiv \phi / \theta_H$$

# Reconciling with Neumann and Dirichlet

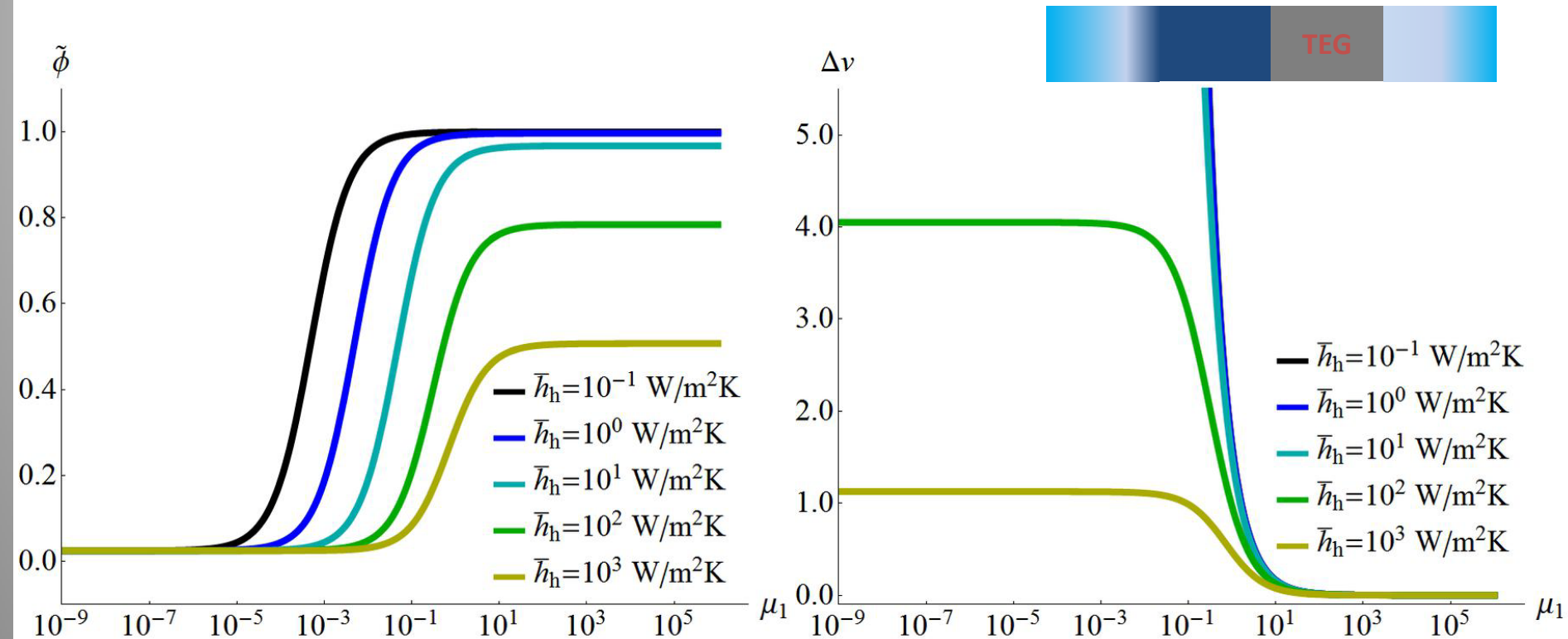


For ideally dissipating cold sides and perfectly insulated heat sources ( $1/\mu_4 = \mu_5 = 0$ ) constant temperature BCs are recovered for  $\mu_1 < 1$  (Dirichlet)

Ideal dissipation conditions show that proper BCs switch upon  $d_H/d_{TE}$  ratio

$$\mu_1 \equiv d_H / d_{TE}$$

# Dissipation efficiency

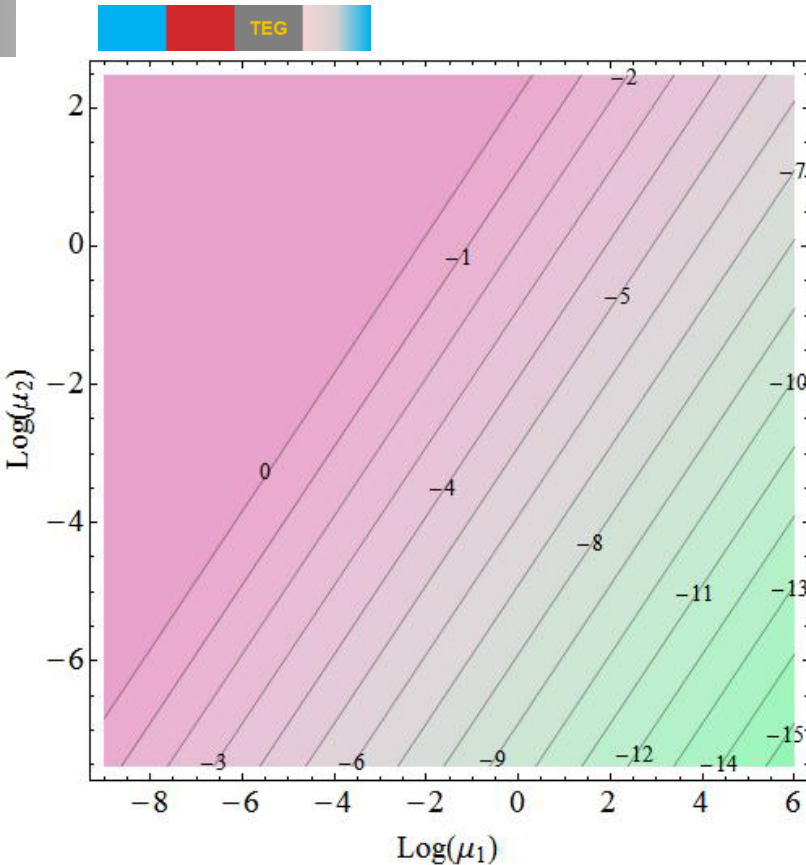


If the hot side is not perfectly insulated (or the heat source strength decreases) constant temperature/heat flow BCs do not apply around  $\mu_1 = 1$ . Since typical  $\mu_1$  for TEGs are between  $10^{-1}$ -  $10^1$  (bulk) and  $10^6$  (micro/nano), application of standard analyses may mislead optimization of leg lengths.

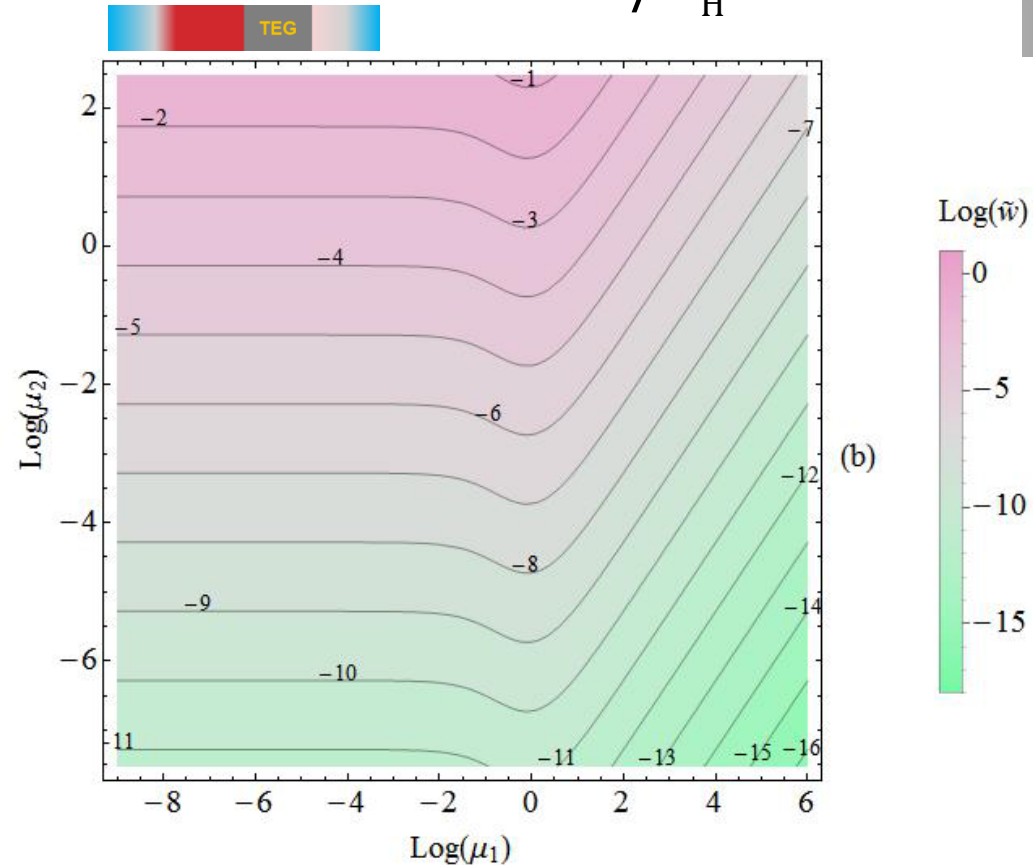


$$\mu_2 \equiv \theta_H d_H / (T_a \kappa_H)$$

$$\tilde{w} \equiv w / \theta_H$$



(a)



(b)

For sub-ideal hot side insulation or low heat source strength, power output remains constant in the  $\mu_1 \rightarrow 0$  limit. Thus, TE legs should fulfill  $\frac{d_{TE}}{d_H} < \mu_1^*$  (relevant for bulk TEGs).

## ZT, PF, $\kappa$ , and leg lengths

The solution of the ODE's reads

$$v_i(\hat{x}) = \sum_{j=0}^2 (\beta_{ji} / \beta_D) \hat{x}^j \quad \text{with} \quad \beta_{ij} = \beta_{ij}(\dots \mu_k \dots)$$

$$\mu_1 \equiv d_H / d_{TE}$$

$$\mu_2 \equiv \theta_H d_H / (T_A \kappa_H) = \theta_H R_H / T_A$$

$$\mu_6 \equiv \kappa_{TE} / \kappa_H$$

$$\mu_3 \equiv \theta_{TE} d_{TE} / (T_A \kappa_{TE}) = \theta_{TE} R_{TE} / T_A$$

$$\mu_4 \equiv \kappa_H / (d_H \bar{h}_h) = 1 / (R_H \bar{h}_h) \quad \mu_5 \equiv \kappa_{TE} / (d_{TE} \bar{h}_c) = 1 / (R_{TE} \bar{h}_c)$$

Since  $\kappa$ 's and  $d$ 's enter the solution independently, the optimization of the TEG geometry will depend on material properties not only through ZT but also through PF and  $\kappa$  separately.

D. Narducci, J. Nanoeng. Nanomanuf. 1 (2011) 63–70.

D. Narducci, Appl. Phys. Lett. 99 (2011) 102104.

## Impact on the design of micro/nanoharvesters

- Dirichlet and Neumann solutions recovered for ideally dissipating systems
- When dissipation is less than ideal, deviations from simplified models may be relevant both for micro and macro-harvesters depending on the characteristics of the heat source (power strength and insulation toward the ambient)
- Expected power outputs are consistent with final device/application requirements ( $10 \mu\text{W}/\text{cm}^2$ )
- From the material scientist viewpoint, once again  $ZT$  and  $\kappa$  should be thought as interdependent parameters.

## Summary

- Two redundant TEG strategies developed:
  - bottom-up, by VLS
  - top-down, by non-critical lithography
- Modeling set up to optimize wire lengths on the heat source
- All technologies are IC-compatible to support integration in the final prototype
- Technologies are flexible enough to be redeployed in other contexts

## The WP2 Team

### CSIC

Luis Fonseca, Carlos Calaza, Marc Salleras, Jaume Esteve, Gonzalo Murillo,  
Carlos Camargo

### IREC

Albert Tarancon, Alex Morata, M. Torrell, G. Gadea, J.D. Santos, M. Fehse

### IMM-CNR

Alberto Roncaglia, Fulvio Mancarella

**University of Milano Bicocca**

Dario Narducci, Laura Zulian



[sinergy-project.eu](http://sinergy-project.eu)

Contact: [luis.fonseca@imb-cnm.csic.es](mailto:luis.fonseca@imb-cnm.csic.es)